

ALI-DPFL: Differentially Private Federated Learning with Adaptive Local Iterations

Xinpeng Ling*, Jie Fu*, Kuncan Wang, Haitao Liu, Zhili Chen†

Shanghai Key Laboratory of Trustworthy Computing, East China Normal University, Shanghai, China

{xpling, jie.fu, kuncan.wang, htliu}@stu.ecnu.edu.cn, zhlcchen@sei.ecnu.edu.cn

Abstract—Federated Learning (FL) is a distributed machine learning technique that allows model training among multiple devices or organizations by sharing training parameters instead of raw data. However, adversaries can still infer individual information through inference attacks (e.g. differential attacks) on these training parameters. As a result, Differential Privacy (DP) has been widely used in FL to prevent such attacks.

We consider differentially private federated learning in a resource-constrained scenario, where both privacy budget and communication rounds are constrained. By theoretically analyzing the convergence, we can find the optimal number of local Differential Privacy Stochastic Gradient Descent (DPSGD) iterations for clients between any two sequential global updates. Based on this, we design an algorithm of Differentially Private Federated Learning with Adaptive Local Iterations (ALI-DPFL). We experiment our algorithm on the MNIST, FashionMNIST and Cifar10 datasets, and demonstrate significantly better performances than previous work in the resource-constraint scenario. Code is available at <https://github.com/KnightWan/ALI-DPFL>.

Index Terms—differential privacy, federated learning, adaptive, convergence analysis, resource constrained

I. INTRODUCTION

In federated learning, each client normally downloads the global model from the center sever, performs local iterations, and uploads the resulted training parameters back to the center sever. The center sever then updates the global model accordingly. The above steps repeat until the global model converges [1]. In this way, the global model reaches convergence by communicating only training parameters instead of raw data. Nevertheless, some studies have shown that federated learning still carries privacy risks. Training parameters, such as gradient values, can be used to recover a portion of the original data [2] or infer whether specific content originates from certain data contributors [3]. Melis et al. [4] also demonstrated that participants’ training data could be leaked by shared models. Therefore, additional measures need to be taken to protect data privacy in federated learning.

Many works [5]–[8] have demonstrated that the technique of differential privacy (DP) could protect machine learning models from unintentional information leakage.

*: These authors contributed equally.

†: Corresponding author.

In differentially private federated learning (DPFL), each client executes a certain number of local stochastic gradient descent with differential privacy (DPSGD) iterations before performing a global aggregation. For each global aggregation, DPFL consumes privacy budget according to the number of local iterations and communicates one round of training parameters, and thus DPFL should be constrained by both the privacy budget and communication rounds. However, current DPFL schemes typically optimize the global model only with the constraint of a limited privacy budget, while overlooking the constraint of communication rounds.

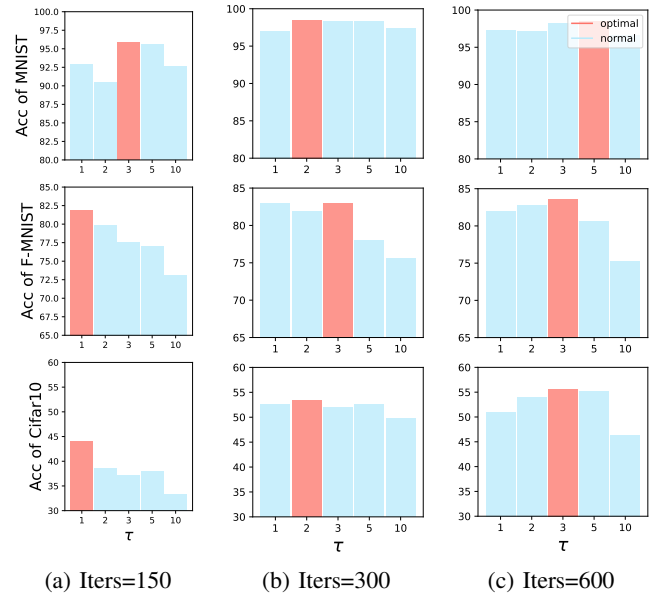


Fig. 1: The test accuracy(%) of fixed τ in different datasets and iterations.

Existing DPFL schemes usually choose empirically a fixed number of local iterations τ for each global update, usually, $\tau = 1$. They treat communication rounds as unlimited, but in practice, the number of communication rounds are often constrained by limited resources such as time and bandwidth. As shown in Fig. 1, the optimal fixed τ value corresponding to the highest accuracy is not a

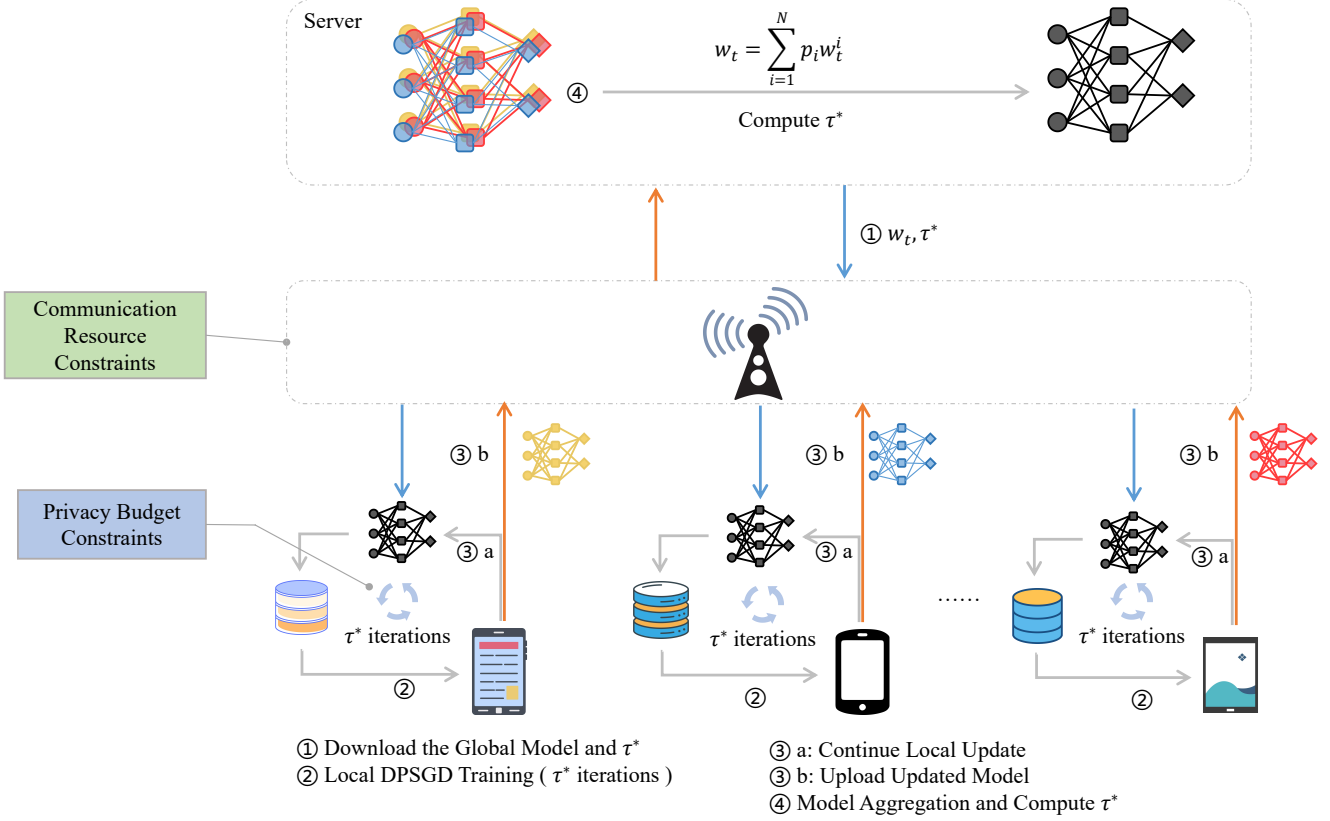


Fig. 2: The Framework of Differentially Private Federated Learning with Adaptive Local Iterations

fixed value across different datasets and iterations. It is also indicated that a fixed τ may fail to achieve satisfactory convergence performances [9]–[11]. Therefore, for the first time, in this paper we focus on finding a DPFL scheme with adaptive local iterations to achieve good performances when both privacy budget and communication rounds are constrained.

Through the convergence analysis, we derive a convergence bound related to the number τ of local iterations. Then, we propose a differentially private federated learning scheme with adaptive local iterations (ALI-DPFL), as shown in Fig. 2, which finds the optimal value (τ^*) in each communication round that minimizes the convergence bound. This value is then used as the number of local iterations in the next round, enabling the algorithm to converge faster under the constraints of privacy budget and communication rounds. The main contributions of this paper are as follows:

- 1) We analyze DPFL convergence under constrained privacy budgets and communication rounds, presenting a novel convergence bound related to the number of local iterations.
- 2) Leveraging this bound, we introduce the ALI-DPFL algorithm, employing adaptive local iterations for

high accuracy and fast convergence in resource-constrained settings.

- 3) Our extensive experiments showcase our approach's superiority over three leading DPFL algorithms across IID and Non-IID data distributions..

The rest of the paper is organized as follows. Section II reviews prior research. Section III introduces the preliminary knowledge. Section IV proposes the ALI-DPFL algorithm through analyzing convergence bound of the DPFL algorithm and proves our algorithm satisfy differential privacy. The experimental results are presented in Section V, followed the conclusion in Section VI.

II. RELATED WORK

A. DPFL

In previous studies, two different types of differential privacy have been incorporated into federated learning to protect privacy: client-level differential privacy (CL-DP) and sample-level differential privacy (SL-DP).

CL-DP. In the CL-DP setting, the model's performance remains stable despite the addition or removal of one client during training [12]. Enayat et al. [13] utilized CL-DP to dynamically adjust the compression rate based on training loss, thereby reducing communication rounds in

federated learning. Zhou et al. [14] explored the impact of local iterations when employing the Laplace mechanism for perturbation.

SL-DP. In the SL-DP setting, each client possesses a set of data samples. Importantly, the addition or removal of a data sample during training has minimal impact on the model's performance [15], [16]. Fu et al. [17] introduced adaptive gradient clipping, tailoring it for different clients and communication rounds based on observed changes in loss values. Raouf et al. [18] leveraged SL-DP to enhance model accuracy by updating only a fixed subset of model weights while leaving others unchanged, thereby reducing bandwidth consumption for both upstream and downstream communication. Kang Wei et al. [19] proposed the adaptive privacy budget allocation. Zhou et al. [20] provided the optimal value for the total local iterations through convergence analysis and analyzed the impact of the total number of iterations on convergence performance and privacy protection. Our work focuses on the SL-DP setting, which is the most popular in the real world.

B. Adaptive local iterations in FL

There are currently numerous adaptive federated learning algorithms aimed at improving model performance in heterogeneous data settings. For example adaptive model aggregation [21], [22], adaptive optimizers [23], adaptive Network Layering [24] and adaptive client sampling [25], etc. Wang et al [11] improved the federated learning algorithm by considering scenarios where clients and the server consume the same type of resources. They achieved faster convergence of the global model under resource constraints by dynamically adjusting local iterations.

Some studies like [11] addressed optimal iteration rounds in FL under limited resources but overlooked differential privacy. Others, such as [14] [20], calculated optimal iteration rounds in DPFL but neglected communication round constraints. This paper, to our knowledge, represents the first attempt to utilize SL-DP convergence analysis to dynamically determine the number of local iterations, achieving rapid convergence.

III. PRELIMINARIES

In the beginning, we list some notations used in this paper in Table I. Symbols that have not been mentioned before will be defined later in the following sections.

A. Differential privacy

Differential privacy is a rigorous mathematical framework that formally defines the privacy loss of data analysis algorithms. Informally, it requires that any changes to a single data point in the training dataset can not cause statistically significant changes in the algorithm's output.

Definition 1: (Differential privacy [26]). (ϵ, δ) -Differential privacy is achieved by a randomized

TABLE I: Summary of main notations

$F(\mathbf{w})$	Global loss function
$F_i(\mathbf{w})$	Local loss function for client i
t	Iteration index
k	Global aggregation index
\mathbf{w}_t^i	Local model parameter at node i at iteration t
\mathbf{w}_t	Global model parameter at iteration t
\mathbf{w}^*	True optimal model parameter that minimizes $F(\mathbf{w})$
η	Gradient descent step size
τ	Number of local update iterations between two global aggregations
τ^*	Dynamic optimal τ in a single round
T	Total number of local iterations
K	Total number of global aggregation, equal to T/τ
p_i	weight of client i
R_s	Maximum communication rounds
R_c	Maximum total local iterations
L	Lipschitz parameter
μ	Strongly convex parameter
σ	Standard deviation of Gaussian distribution
d	The dimension of model
C	Clipping bound
q	Sampling rate of batch
$\ \cdot\ $	L_2 -norm

mechanism $\mathcal{M} : \mathcal{X} \rightarrow \mathcal{R}$ if, for any two neighboring databases $\mathcal{D}_i, \mathcal{D}'_i \in \mathcal{X}$ that differ in only a single entry, and $\forall \mathcal{S} \subseteq \text{Range}(\mathcal{R})$,

$$\Pr[\mathcal{M}(\mathcal{D}_i) \in \mathcal{S}] \leq e^\epsilon \Pr[\mathcal{M}(\mathcal{D}'_i) \in \mathcal{S}] + \delta \quad (1)$$

B. Differentially private stochastic gradient descent

Differentially Private Stochastic Gradient Descent (DPSGD) stands as a widely embraced deep learning algorithm offering privacy guarantees [15], [27]–[30]. Specifically, at each iteration t , a batch of data \mathcal{B}_t is sampled from the dataset using a sampling rate q . Subsequently, for each batch, s is a sample thereof. Following the clipping of per-sample gradients, Gaussian noise with a mean of 0 is incorporated into the gradients in the subsequent step:

$$\begin{aligned} \bar{g}_t(s) &= \text{clip}(\nabla F(\mathbf{w}_t, s)) \\ &= \nabla F(\mathbf{w}_t, s) / \max\left(1, \frac{\|\nabla F(\mathbf{w}_t, s)\|}{C}\right) \end{aligned} \quad (2)$$

$$\tilde{g}_t = \frac{1}{|\mathcal{B}_t|} \left(\sum_{s \in \mathcal{B}_t} \bar{g}_t(s) + \mathcal{N}(0, \sigma^2 C^2 \mathbf{I}_d) \right) \quad (3)$$

Here, σ represents the noise multiplier, while C denotes the clipping bound. Subsequently, gradient descent is executed based on the batch-averaged gradients. The initial models being randomly generated and independent of the sample data, combined with the batch-averaged gradients adhering to differential privacy, ensures that the resulting models also adhere to differential privacy, attributable to the post-processing property [31].

Algorithm 1: Federated Learning with Differential Privacy

Input: loss function $F(\mathbf{w})$. Parameters: learning rate η , noise multiplier σ , local iterations τ , clipping bound C , sampling rate q

Output: the final trained model $\mathbf{w}(K)$

- 1 Initialize $k = 0$, $\mathbf{w}_0 = \text{Initial}();$
- 2 **while** $k < K$ **do**
- 3 **for** $i \in [1, 2, \dots, N]$ **parallel do**
- 4 **for** $j \in [1, 2, \dots, \tau]$ **do**
- 5 $t = (k-1)\tau + j;$
- 6 Sample randomly a batch \mathcal{B}_t^i with sampling rate q ;
- 7 **for** $s \in \mathcal{B}_t^i$ **do**
- 8 $g_t^i(s) \leftarrow \nabla F_i(\mathbf{w}_t^i, s);$
- 9 $\bar{g}_t^i(s) \leftarrow g_t^i(s) / \max(1, \frac{\|g_t^i(s)\|}{C});$
- 10 $\tilde{g}_t^i \leftarrow \sum_{s \in \mathcal{B}_t^i} \bar{g}_t^i(s) + \mathcal{N}(0, \sigma^2 C^2 \mathbf{I}_d);$
- 11 $\mathbf{w}_{t+1}^i = \mathbf{w}_t^i - \eta \cdot \frac{\tilde{g}_t^i}{|\mathcal{B}_t^i|};$
- 12 Receive \mathbf{w}_{t+1}^i ;
- 13 $k = k + 1;$
- 14 $\mathbf{w}(k) = \sum_{i=1}^N p_i \mathbf{w}_{t+1}^i;$
- 15 Broadcast $\mathbf{w}(k)$ to each client ;
- 16 **return** $\mathbf{w}(K)$

C. Federated Learning with Differential Privacy

In a typical federated learning system, a server and N clients form the fundamental components [1] [32]. Each client, denoted as C_i , maintains a local database \mathcal{D}_i , where $i \in \{1, 2, \dots, N\}$. The quantity $|\mathcal{D}_i|$ signifies the size of the dataset at client i , and the total dataset size is denoted as $|\mathcal{D}| = \sum_{i=1}^N |\mathcal{D}_i|$. Let $p_i \triangleq \frac{|\mathcal{D}_i|}{|\mathcal{D}|}$ represent the weight of client i . The server's objective is to learn a model using data distributed across the N clients. Each active client engaged in local training endeavors to discover a vector \mathbf{w} that represents the neural network model minimizing a specific loss function. Subsequently, the server aggregates the weights from the N clients, a process that can be expressed as:

$$\mathbf{w}(k) = \sum_{i=1}^N p_i \mathbf{w}_t^i \quad (4)$$

Here, \mathbf{w}_t^i signifies the parameter vector acquired from client i at iteration t , while $\mathbf{w}(k)$ denotes the server-aggregated parameter vector at communication round k . The objective is to minimize $F(\mathbf{w})$, in other words, to seek:

$$\mathbf{w}^* \triangleq \arg \min F(\mathbf{w}) \quad (5)$$

The function $F(\cdot)$ is defined as follows:

$$F(\mathbf{w}) \triangleq \sum_{i=1}^N p_i F_i(\mathbf{w}) \quad (6)$$

Here, $F_i(\cdot)$ represents the local loss function of client i .

As depicted in Algorithm 1, the differentiating factor between the DPFL algorithm and traditional federated learning algorithms resides in the utilization of DPSGD instead of SGD. Specifically, at line 9, the DPFL algorithm executes per-sample clipping, and at line 10, it introduces noise to the clipped gradients.

IV. ALI-DPFL ALGORITHM

In this section, we introduce our ALI-DPFL algorithm, which is based on the insights gleaned from the convergence analysis. In Section IV-A, we conducted a convergence analysis of the traditional DPFL algorithm to investigate the relationship between the convergence upper bound and τ , resulting in Equation (7). Leveraging the outcomes of the convergence analysis, we derived Lemma 1 and Lemma 2. Subsequently, in Section IV-B, we outline the workflow of ALI-DPFL. Furthermore, in Section IV-C, we constructed Algorithm 2 based on Lemma 1 and Lemma 2. Finally, in Section IV-D, we demonstrated that Algorithm 2 satisfies the conditions for differential privacy.

A. Motivation: Convergence Analysis of DPFL

To investigate the impact of τ on the convergence rate, we delve into the convergence of Algorithm 1 and draw insights on selecting the optimal local iteration count τ^* based on the convergence upper bound. Prior to substantiating this, we establish several assumptions:

Assumption 1: F_1, \dots, F_N are all L-smooth [33]: for all \mathbf{v} and \mathbf{w} , $F_i(\mathbf{v}) \leq F_i(\mathbf{w}) + (\mathbf{v} - \mathbf{w})^T \nabla F_i(\mathbf{w}) + \frac{L}{2} \|\mathbf{v} - \mathbf{w}\|^2$.

Assumption 2: F_1, \dots, F_N are all μ -strongly convex [34]: for all \mathbf{v} and \mathbf{w} , $F_i(\mathbf{v}) \geq F_i(\mathbf{w}) + (\mathbf{v} - \mathbf{w})^T \nabla F_i(\mathbf{w}) + \frac{\mu}{2} \|\mathbf{v} - \mathbf{w}\|^2$.

Assumption 3: The L_2 norm of stochastic gradients is uniformly bounded by the clipping bound [35], i.e., $\|\nabla F_i(\mathbf{w}_t^i, s)\| \leq C$ for all $i = 1, \dots, N$, $t = 1, \dots, T$ and $s \in \mathcal{B}^i$.

Theorem 1: Given the aforementioned assumptions, we derive the convergence upper bound for Algorithm 1 as follows:

$$\mathbb{E}[F(\mathbf{w}_t)] - F^* \leq h(\tau), \quad (7)$$

where:

$$h(\tau) \triangleq \frac{L(2 + \eta\mu) \left(C^2 + \frac{\sigma^2 C^2 d}{\hat{B}^2} \right)}{2T} \tau^2 + \frac{L\Delta_1 - 2L(2 + \eta\mu) \left(C^2 + \frac{\sigma^2 C^2 d}{\hat{B}^2} \right)}{2T} \tau + \frac{L \left((2 + \eta\mu) \left(C^2 + \frac{\sigma^2 C^2 d}{\hat{B}^2} \right) + \frac{4}{\mu^2} + 3C^2 + \frac{2\Gamma}{\eta} + \frac{\sigma^2 C^2 d}{\hat{B}^2} \right)}{2T}.$$
(8)

Here $\frac{1}{\hat{B}} \triangleq \max_{i,t} \mathbb{E} \frac{1}{|\mathcal{B}_i^t|}$, $\Delta_1 = \mathbb{E} \|\bar{\mathbf{w}}_1 - \mathbf{w}^*\|^2$. $\Gamma = F^* - \sum_{i=1}^N p_i F_i^*$, which is consistent with [36], where a larger value of Γ indicates that the data among different clients is more non-IID.

Proof Sketch: We explore the relationship between $\mathbb{E} \|\bar{\mathbf{w}}_{t+1} - \mathbf{w}^*\|^2$ and $\mathbb{E} \|\bar{\mathbf{w}}_t - \mathbf{w}^*\|^2$, subsequently employing mathematical induction to establish an upper bound for $\mathbb{E} \|\mathbf{w}_t - \mathbf{w}^*\|^2$. Ultimately, leveraging Assumption 1, we derive (7). For a comprehensive proof, please refer to Appendix¹A.

Lemma 1: Disregarding the limitation on the number of communication rounds, $\tau = 1$ yields the fastest convergence.

Proof: Observing Equation (8), we note that $h(\tau)$ forms a quadratic function of τ . The minimum value of $h(\tau)$ is attained when:

$$\tau_0 = 1 - \frac{\Delta_1}{2(2 + \eta\mu) \left(C^2 + \frac{\sigma^2 C^2 d}{\hat{B}^2} \right)}$$

As $0 < \tau_0 < 1$, we conclude that $h(\tau)$ achieves its minimum value at $\tau = 1$.

Lemma 2: Considering the constraint on the number of communication rounds, we can derive an optimal τ^* :

$$\tau^* = \sqrt{1 + \frac{\frac{4}{\mu^2} + 3C^2 + 2\Gamma T \mu + \frac{\sigma^2 C^2 d}{\hat{B}^2}}{(2 + \frac{1}{T}) \left(C^2 + \frac{\sigma^2 C^2 d}{\hat{B}^2} \right)}}$$
(9)

Proof: The number of required communication rounds is determined by $\frac{T}{\tau}$. As this value is constant, we have:

$$h(\tau) = \frac{\tau}{T} \cdot G(\tau),$$
(10)

where:

$$G(\tau) \triangleq \frac{L(2 + \eta\mu) \left(C^2 + \frac{\sigma^2 C^2 d}{\hat{B}^2} \right)}{2} \tau + \frac{L\Delta_1 - 2L(2 + \eta\mu) \left(C^2 + \frac{\sigma^2 C^2 d}{\hat{B}^2} \right)}{2} + \frac{L \left((2 + \eta\mu) \left(C^2 + \frac{\sigma^2 C^2 d}{\hat{B}^2} \right) + \frac{4}{\mu^2} + 3C^2 + \frac{2\Gamma}{\eta} + \frac{\sigma^2 C^2 d}{\hat{B}^2} \right)}{2\tau}.$$
(11)

¹Due to the limited space, please access the appendix at arXiv: <https://arxiv.org/abs/2308.10457>

When $\frac{T}{\tau}$ is a constant number, we minimize $G(\tau)$ to minimize $h(\tau)$. We observe that $G(\tau)$ is a parabolic function of τ , and choosing excessively large or small values of τ would result in a large convergence bound, detrimental to the convergence of the algorithm. By minimizing $G(\tau)$, we obtain τ^* as given in Equation (9).

B. Overview

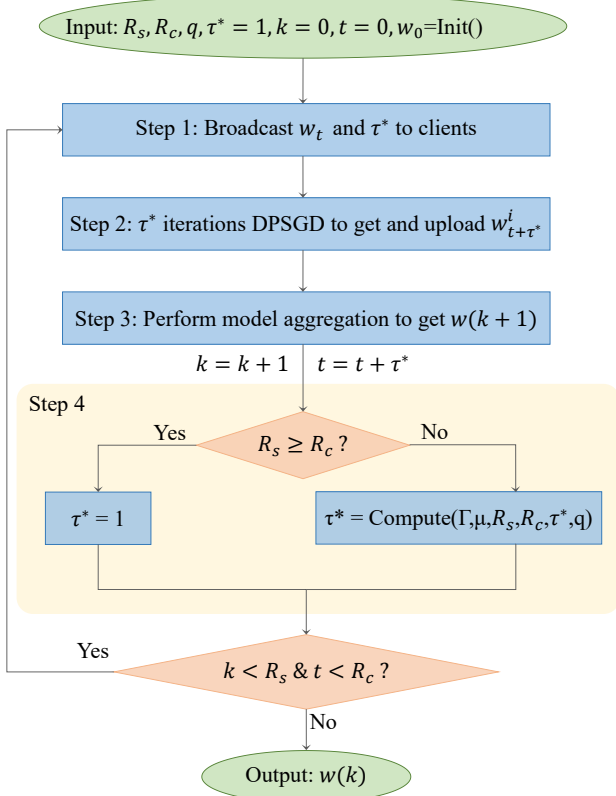


Fig. 3: Workflow of ALI-DPFL

As previously discussed, a fixed value of τ could impede the algorithm's rapid convergence. Hence, it is imperative to compute the optimal τ^* at each communication round. The process for computing τ^* is delineated in Figure 3.

- **step 1:** The server disseminates the aggregated model \mathbf{w}_t acquired from step 3 and the optimal local iterations τ^* obtained from step 4 to the clients.
- **step 2:** Each client concurrently executes τ^* iterations of DPSGD and uploads $\mathbf{w}_{t+\tau^*}^i$ to the central server.
- **step 3:** The server performs weighted aggregation on all models uploaded by the clients to derive the new server model for the subsequent round.
- **step 4:** The server computes τ^* . If $R_s \geq R_c$, then $\tau^* = 1$; otherwise, τ^* is computed using Equation (9). The parameters required by Equation (9) are calculated as follows:

1) Compute the strongly convex parameter as per Assumption 2:

$$\mu \leftarrow \sum_{i=1}^N p_i \frac{\|\nabla F_i(\mathbf{w}_t^i) - \nabla F_i(\mathbf{w}_t)\|}{\|\mathbf{w}_t^i - \mathbf{w}_t\|}$$

2) Calculate T based on R_s, R_c , and the previous round's τ^* :

$$T \leftarrow \min\{R_s \cdot \tau^*, R_c\}$$

3) Determine \hat{B} as per the definition:

$$\hat{B} \leftarrow \min_i q \cdot |\mathcal{D}_i|$$

C. Our Algorithm

Algorithm 2: Adaptive Local Iterations Differentially Private Federated Learning

Input: loss function $F(\mathbf{w})$. Parameters: learning rate η , noise multiplier σ , privacy budget ϵ , local iterations τ , clipping bound for training C , sampling rate q , heterogeneous parameter Γ , maximum global rounds R_s , maximum total iterations R_c

Output: the final trained model $\mathbf{w}(k)$

1 Initialize $k = 0, t = 0, \mathbf{w}_0 = \text{Initial}()$;
2 **while** $k < R_s$ and $t < R_c$ **do**
3 **for** $i \in [1, 2, \dots, N]$ **parallel do**
4 **for** $j \in [1, 2, \dots, \tau^*]$ **do**
5 $t = t + 1$;
6 Sample randomly a batch \mathcal{B}_t^i with sampling rate q ;
7 **for** $s \in \mathcal{B}_t^i$ **do**
8 $g_t^i(s) \leftarrow \nabla F_i(\mathbf{w}_t^i, s)$;
9 $\bar{g}_t^i(s) \leftarrow g_t^i(s) / \max(1, \frac{\|g_t^i(s)\|}{C})$;
10 $\bar{g}_t^i \leftarrow \sum_{s \in \mathcal{B}_t^i} \bar{g}_t^i(s) + \mathcal{N}(0, \sigma^2 C^2 \mathbf{I}_d)$;
11 $\mathbf{w}_{t+1}^i = \mathbf{w}_t^i - \eta \cdot \frac{\bar{g}_t^i}{|\mathcal{B}_t^i|}$;
12 Receive \mathbf{w}_{t+1}^i ;
13 $k = k + 1$;
14 $\mathbf{w}(k) = \sum_{i=1}^N p_i \mathbf{w}_{t+1}^i$;
15 **if** $R_s \geq R_c$ **then**
16 $\tau^* = 1$;
17 **else**
18 $\tau^* = \text{Compute}(\Gamma, \mu, R_s, R_c, \tau^*, q)$ according to (9);
19 Broadcast $\mathbf{w}(k), \tau^*$ to each client ;
20 **return** $\mathbf{w}(k)$

Our objective is to adapt the value of τ to minimize either (8) or (11). This adjustment aims to bring \mathbf{w}_t as close as feasible to \mathbf{W}^* , consequently facilitating swift convergence within resource constraints. As depicted in Algorithm 2, the

Algorithm 3: Compute R_c

Input: target privacy budget ϵ, δ , sampling rate q , noise multiplier σ

1 Initialize $T_l = 0, T_r = 1e + 10, \epsilon_m = 0$;
2 **while** $\epsilon_m - \epsilon < 0.01$ **do**
3 $T_m = \frac{T_l + T_r}{2}$;
4 $\epsilon_m \leftarrow \text{Compute privacy loss}(q, \sigma, T_m, \delta)$ by Theorem 2 ;
5 **if** $\epsilon_m > \epsilon$ **then**
6 $T_r = T_m$
7 **else**
8 $T_l = T_m$
9 **return** T_l

disparity between ALI-DPFL and DPFL algorithms lies in the necessity to compute τ^* instead of relying on a fixed τ .

- **lines 3-11 (Local DPSGD):** During this phase, N clients engage in parallel training. Initially, they receive \mathbf{w}_t and τ^* , then proceed with τ^* rounds of DPSGD iterations. In **line 6**, a sampling rate q is utilized for Poisson sampling, drawing inspiration from [37], to obtain the data batch \mathcal{B}_t^i . Following this, in **lines 8-10**, the gradients of each sample within a single local iteration are clipped, then the gradients of the entire batch are summed, noise is added, and finally, the result is divided by the batch size $|\mathcal{B}_t^i|$. Subsequently, in **line 11**, gradient descent is performed locally using the processed gradients, and the updated model is uploaded to the server.
- **line 14 (Aggregation):** Upon reception of models from each client, Algorithm 2 proceeds to average the models based on weights.
- **lines 15-18 (Compute τ^*):** According to Lemma 1 and Lemma 2, the approach to obtaining τ^* differs. When R_s (server resources, i.e., maximum communication rounds) is greater than or equal to R_c (client resources, i.e., maximum total local iterations), as per Lemma 1, it is established that $\tau^* = 1$. Conversely, when R_s is less than R_c , τ^* is computed based on Equation (9).

The value of R_s can be pre-defined or controlled using methods such as time thresholds or communication bandwidth limits. Furthermore, the determination of R_c can be achieved through Algorithm 3 when establishing the parameters for differential privacy. Specifically, by defining the target privacy budget ϵ , sampling rate q , and noise multiplier σ , the algorithm can obtain the corresponding total iteration rounds R_c through a binary search.

D. Privacy Analysis

Since each client's locally trained data samples share the same sampling rate, noise multiplier, and local iterations in each round, it follows that each client incurs an identical privacy loss in every round. Our analysis of each client's privacy loss is conducted from the viewpoint of an individual client. Subsequently, we investigate the privacy budget for the i -th client (the privacy loss analysis for the other clients follows the same procedure).

Theorem 2: (DP Privacy Loss of Algorithm 2). After T local iterations, the i -th client DP Privacy budget of Algorithm 2 satisfies:

$$(\epsilon_T^i, \delta) = \left(\sum_{t=0}^T \frac{1}{\alpha-1} \sum_{k=0}^{\alpha} \binom{\alpha}{k} (1-q)^{\alpha-k} q^k \exp\left(\frac{k^2 - k}{2\sigma^2}\right) + \frac{\log 1/\delta}{\alpha-1}, \delta \right) \quad (12)$$

where q is the sampling rate, σ is noise multiplier and any integer $\alpha \geq 2$.

proof. Our privacy loss calculation is based on RDP [37]. Initially, we utilize the sampling Gaussian theorem of RDP to compute the privacy cost of each round. Subsequently, we apply advanced combination techniques of RDP to aggregate the privacy cost across multiple rounds. Finally, we convert the resulting RDP privacy to DP.

Definition 2: (RDP privacy budget of SGM [38]). Let $SG_{q,\sigma}$, be the Sampled Gaussian Mechanism for some function f . If f has sensitivity 1, $SG_{q,\sigma}$ satisfies (α, R) -RDP whenever

$$R \leq \frac{1}{\alpha-1} \log \max(A_\alpha(q, \sigma), B_\alpha(q, \sigma)) \quad (13)$$

where:

$$\begin{cases} A_\alpha(q, \sigma) \triangleq \mathbb{E}_{z \sim \vartheta_0} [(\vartheta(z)/\vartheta_0(z))^\alpha] \\ B_\alpha(q, \sigma) \triangleq \mathbb{E}_{z \sim \vartheta} [(\vartheta_0(z)/\vartheta(z))^\alpha] \end{cases} \quad (14)$$

with $\vartheta_0 \triangleq \mathcal{N}(0, \sigma^2)$, $\vartheta_1 \triangleq \mathcal{N}(1, \sigma^2)$ and $\vartheta \triangleq (1-q)\vartheta_0 + q\vartheta_1$

Further, it holds $\forall (q, \sigma) \in (0, 1], \mathbb{R}^{+*}, A_\alpha(q, \sigma) \geq B_\alpha(q, \sigma)$. Thus, $SG_{q,\sigma}$ satisfies $\left(\alpha, \frac{1}{\alpha-1} \log (A_\alpha(q, \sigma))\right)$ -RDP.

Finally, [38] describes a procedure to compute $A_\alpha(q, \sigma)$ depending on integer α .

$$A_\alpha = \sum_{k=0}^{\alpha} \binom{\alpha}{k} (1-q)^{\alpha-k} q^k \exp\left(\frac{k^2 - k}{2\sigma^2}\right) \quad (15)$$

Definition 3: (Composition of RDP [37]). For two randomized mechanisms f, g such that f is (α, R_1) -RDP and g is (α, R_2) -RDP the composition of f and g which is defined as (X, Y) (a sequence of results), where $X \sim f$ and $Y \sim g$, satisfies $(\alpha, R_1 + R_2) - RDP$

From Definition 2 and Definition 3, the following Lemma 3 is obtained.

Lemma 3: Given the sampling rate q for each round of the local dataset and σ as the noise factor, the total RDP privacy loss of the i -th client for local iterations T for any integer $\alpha \geq 2$ is:

$$\epsilon'(\alpha)_T^i = \sum_{t=0}^T \frac{1}{\alpha-1} \sum_{k=0}^{\alpha} \binom{\alpha}{k} (1-q)^{\alpha-k} q^k \exp\left(\frac{k^2 - k}{2\sigma^2}\right) \quad (16)$$

Definition 4: (Translation from RDP to DP [37]). if a randomized mechanism $f : D \rightarrow \mathbb{R}$ satisfies (α, ϵ) -RDP , then it satisfies $(\epsilon + \frac{\log 1/\delta}{\alpha-1}, \delta)$ -DP where $0 < \delta < 1$.

By Lemma 3 and Definition 4, Theorem 2 is proved.

V. EXPERIMENT

We carried out a series of comparative experiments on the MNIST, FashionMnist, and Cifar10 datasets. The results of these experiments illustrate that our ALI-DPFL algorithm consistently delivers outstanding performance, enhancing accuracy across various ratios between R_s and R_c .

A. setup

1) *baseline*: We compared the ALI-DPFL algorithm with three different baselines:

- **FedAvg [1]+DP**: FedAvg, as the earliest Federated Learning algorithm, was executed with a fixed τ . We replace SGD with DPSGD to ensure privacy protection while setting $\tau = \{1, 2, 3, 5, 10\}$ as the baselines.
- **PE-DPFL [39]**: This algorithm introduces a regularization term to the objective function and directly adds noise to the model before uploading. For our comparative experiments, we utilized hyperparameters epoch = 1 and $\tau = 3$.
- **Adap DP-FL [17]**: This algorithm dynamically adjusts the value of σ based on whether the loss has decreased within four rounds. Similarly, for our comparative experiments, we employed hyperparameters epoch = 1 and $\tau = 3$.

2) *dataset*: In our study, we conducted experiments on various R_s and R_c ratios under independent and identically distributed (IID) as well as non-independent and identically distributed (Non-IID) data distributions. We employed the following three real datasets: MNIST [40], FashionMNIST [41] and Cifar10 [42].

3) *default parameters*: With a learning rate of $\eta = 0.5$, we conducted experiments using ALI-DPFL with convolutional neural networks. For MNIST and FMNIST, the neural network structure is detailed in Table ??, while for Cifar10, the neural network structure is outlined in Table ???. We established the sampling rate q at 0.015, with 10 clients participating in each training iteration. To simulate data heterogeneity, we employed a real heterogeneous setting [43] controlled by a Dirichlet distribution denoted as $\text{Dir}(\beta)$, where smaller β values indicate higher data heterogeneity. We set the default value to $\beta = 0.05$ [10]

TABLE II: (Small R_s) The average accuracy(%) on MNIST, Fashion MNIST and Cifar10.

Datasets	$R_s = 2R_c, \epsilon = 1.55$			$R_s = R_c, \epsilon = 1.75$			$R_s = \frac{1}{2}R_c, \epsilon = 2$			$R_s = \frac{1}{5}R_c, \epsilon = 2.75$		
	MNIST	FMNIST	Cifar10	MNIST	FMNIST	Cifar10	MNIST	FMNIST	Cifar10	MNIST	FMNIST	Cifar10
PE-DPFL	80.12	79.81	38.22	96.02	80.91	42.61	97.42	82.15	48.98	97.99	83.92	51.90
Adap DP-FL	85.83	80.11	39.12	94.21	81.31	46.12	95.41	81.30	47.39	96.98	82.05	49.96
$\tau = 1^2$	85.65	79.98	39.33	96.01	81.94	46.27	95.06	81.64	47.27	97.08	82.14	47.20
$\tau = 2$	81.26	79.66	32.55	95.99	81.48	42.91	96.77	83.20	50.79	97.99	82.90	50.96
$\tau = 3$	78.63	78.55	31.23	95.21	81.26	41.33	97.51	82.60	49.28	98.15	83.60	52.85
$\tau = 5$	77.62	77.68	26.38	95.14	79.64	41.06	97.49	82.25	47.62	97.96	82.45	53.14
$\tau = 10$	76.65	75.32	23.46	91.05	76.32	40.20	95.18	78.23	44.38	96.42	76.78	48.30
ALI-DPFL	86.10	80.17	39.82	96.25	82.02	46.32	97.58	83.44	51.92	98.25	84.07	53.54

 TABLE III: (Medium R_s) The average accuracy(%) on MNIST, Fashion MNIST and Cifar10.

Datasets	$R_s = 2R_c, \epsilon = 1.75$			$R_s = R_c, \epsilon = 2$			$R_s = \frac{1}{2}R_c, \epsilon = 2.5$			$R_s = \frac{1}{5}R_c, \epsilon = 3.75$		
	MNIST	FMNIST	Cifar10	MNIST	FMNIST	Cifar10	MNIST	FMNIST	Cifar10	MNIST	FMNIST	Cifar10
PE-DPFL	96.04	78.11	38.22	96.99	83.05	53.61	98.02	81.69	52.83	98.08	83.31	54.21
Adap DP-FL	93.08	80.21	43.53	97.12	82.70	55.21	97.02	82.88	52.77	97.42	82.05	52.32
$\tau = 1$	96.12	81.84	44.06	97.23	83.71	54.96	96.91	82.96	52.66	97.33	81.99	51.00
$\tau = 2$	95.46	79.88	38.63	96.57	82.84	54.33	98.38	81.94	53.41	97.15	82.83	53.92
$\tau = 3$	94.82	77.51	37.20	95.46	82.61	53.08	98.23	82.99	52.04	98.23	83.57	55.60
$\tau = 5$	93.54	76.96	38.02	94.49	80.46	53.91	98.33	77.96	52.63	98.52	80.70	55.17
$\tau = 10$	92.68	73.12	33.25	93.31	79.56	51.78	97.31	75.56	49.72	96.65	75.29	46.32
ALI-DPFL	96.14	81.86	44.12	97.59	83.88	55.01	98.15	83.58	53.86	98.82	84.31	55.67

 TABLE IV: (Large R_s) The average accuracy(%) on MNIST, Fashion MNIST and Cifar10.

Datasets	$R_s = 2R_c, \epsilon = 2$			$R_s = R_c, \epsilon = 2.5$			$R_s = \frac{1}{2}R_c, \epsilon = 3.25$			$R_s = \frac{1}{5}R_c, \epsilon = 5.25$		
	MNIST	FMNIST	Cifar10	MNIST	FMNIST	Cifar10	MNIST	FMNIST	Cifar10	MNIST	FMNIST	Cifar10
PE-DPFL	92.94	81.81	42.22	97.43	81.90	50.31	98.12	81.84	52.91	98.12	83.94	56.70
Adap DP-FL	94.32	80.01	50.13	95.12	81.21	55.41	98.45	82.32	53.32	98.08	83.85	56.86
$\tau = 1$	94.92	82.53	49.99	97.57	84.02	56.41	97.93	83.39	54.33	96.98	83.70	53.37
$\tau = 2$	94.46	81.49	44.54	97.46	82.92	50.11	98.58	83.46	54.96	97.89	83.72	55.56
$\tau = 3$	92.98	81.56	41.14	97.32	82.73	50.59	98.61	83.24	53.08	98.11	83.75	56.84
$\tau = 5$	92.86	78.48	41.25	97.49	82.50	50.47	98.85	81.67	53.91	98.33	81.72	55.21
$\tau = 10$	91.98	75.32	38.85	96.58	81.72	47.98	97.21	79.65	51.78	97.42	81.25	54.55
ALI-DPFL	95.22	82.58	50.14	97.74	84.19	56.76	98.84	83.25	55.17	98.82	84.58	57.25

[43] and $\Gamma = 10$. We conducted experiments using a neural network with 2 convolutional layers and 2 fully connected layers on three datasets.

B. Performance

In Lemma 1, we highlighted that $\tau = 1$ represents the optimal choice for achieving the fastest convergence of the algorithm when the constraint of communication rounds is not taken into account. Previous studies analyzing convergence have primarily focused on the relationship between accuracy and the number of local iterations [36], [44]–[46]. We have observed that the convergence bound consistently incorporates accuracy and the number of local iterations in the denominator. Holding accuracy constant, more iterations result in a smaller convergence bound. Selecting $\tau = 1$ maximizes the number of iterations, aligning with our observation in Lemma 1. Based on this insight, we designed the following experiments:

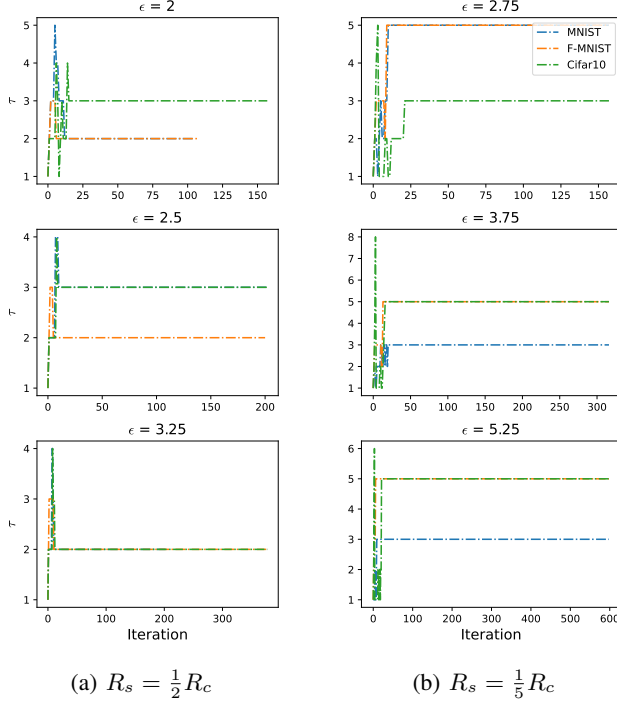
Condition I: When $R_s \geq R_c$, as per the aforementioned analysis, setting all values in the τ list to 1 yields the best model performance. Hence, we verified two cases: $R_s = R_c$ and $R_s = 2R_c$, under three fixed conditions of R_s .

²All fixed τ methods source from FedAvg+DP.

Condition II: When $R_s < R_c$, setting all values in the τ list to 1 does not fully utilize local resources. Therefore, we examined two cases: $R_s = \frac{1}{2}R_c$ and $R_s = \frac{1}{5}R_c$, under three fixed conditions of R_s .

In our experiments, we compared the ALI-DPFL method with the fixed τ method, FedAvg [1]+DP, PE-DPFL [39], and Adap DP-FL [17]. We conducted experiments for four different ratios: $R_s = R_c$, $R_s = 2R_c$, $R_s = \frac{1}{2}R_c$, and $R_s = \frac{1}{5}R_c$, under three conditions: $R_s = \{158, 231, 317\}$. To accommodate the four cases of $R_s = n \cdot R_c$ and the three values of $R_s = \{158, 231, 317\}$, we selected the following privacy budgets: $\epsilon = \{1.55, 1.75, 2, 2.5, 2.75, 3.25, 3.75, 5.25\}$. These values support $\{79, 177, 317, 598, 775, 1123, 1585, 2990\}$ iterations, approximately meeting the experimental requirements.

As depicted in Tables II, III, and IV, we evaluated the performance of these methods under Non-IID conditions (utilizing a Dirichlet distribution parameter of 0.05). Each entry in the tables represents the average result obtained after three replications. Our findings indicate that in the majority of cases, our method outperforms the other methods.



(a) $R_s = \frac{1}{2}R_c$

(b) $R_s = \frac{1}{5}R_c$

Fig. 4: Adaptive τ value when $R_s < R_c$.

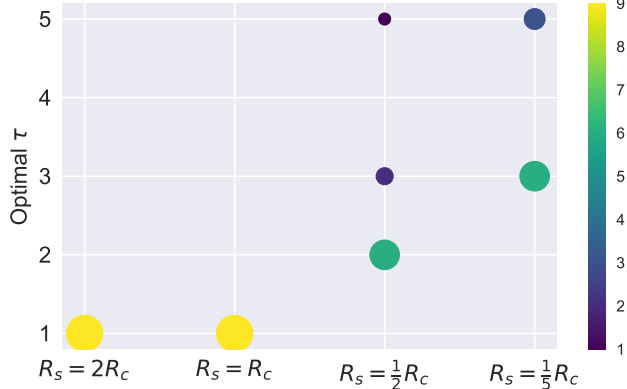


Fig. 5: The frequencies of optimal fixed τ in Table II, III, IV

C. Exploration the reason of outperform

We counted the optimal τ values for each resource ratio in the fixed τ algorithm and illustrated them in Fig. 5. Our analysis revealed that when $R_s = \frac{1}{2}R_c$, the optimal τ values predominantly clustered around 2 and 3. Similarly, when $R_s = \frac{1}{5}R_c$, the optimal τ values were mainly concentrated in 3 and 5.

Subsequently, we depicted the τ lists for the ALI-DPFL algorithm where $R_s < R_c$ in Table II, III, and IV in Fig. 4. Our observations indicated that initially, the value of τ^* exhibited fluctuations, but after several iterations, it stabilized to an appropriate τ . Furthermore, when $R_s = \frac{1}{2}R_c$,

the values in the τ list stabilized around 2 and 3, while for $R_s = \frac{1}{5}R_c$, the values in the τ list stabilized around 3 and 5. These findings suggest that ALI-DPFL effectively identifies the τ values conducive to rapid model convergence under varying resource ratios.

D. Robustness with heterogeneous data

TABLE V: The average accuracy(%) on heterogeneous setting at FasionMNIST dataset, $R_s = \frac{1}{3}$, $\epsilon = 2$.

	IID	Dir(0.05)	Dir(0.5)	Dir(1)
FedAvg+DP	88.23	83.96	84.01	84.32
PE-DPFL	83.21	81.06	82.56	83.00
Adap DP-FL	87.12	83.58	83.62	84.05
$\tau = 1$	84.56	80.92	81.01	82.77
$\tau = 2$	86.12	82.15	84.61	84.88
$\tau = 3$	89.46	84.45	84.89	85.82
$\tau = 5$	83.30	80.62	81.21	82.05
$\tau = 10$	76.56	73.56	74.06	74.51
ALI-DPFL	89.62	84.85	85.45	86.12

To showcase the robustness of Algorithm 2 in Non-IID data settings, we conducted experiments utilizing different data partitioning methods on the FashionMNIST dataset, with $R_s = \frac{1}{3}R_c$ and $\epsilon = 2$. As depicted in Table V, the performance of the ALI-DPFL algorithm surpassed that of other methods in the cases of IID, Dir(0.05), Dir(0.5), and Dir(1). Correspondingly, we set the parameter Γ to 0, 10, 5, and 1.

VI. CONCLUSION

In this paper, we present an algorithm of Differential Private Federated Learning with Adaptive Local Iterations (ALI-DPFL), in the scenario where privacy budget and communication rounds are constrained. Through a theoretical convergence analysis of DPFL, we derive a convergence bound depending on the number of local iterations τ , and improve the performance of federated learning with differential privacy by dynamically finding the optimal τ . We formally prove the privacy of the proposed algorithm with the RDP technique, and conduct extensive experiments to demonstrate that ALI-DPFL significantly outperforms existent schemes in the resource-constraint scenario.

ACKNOWLEDGMENTS

This work is supported by the Natural Science Foundation of Shanghai (Grant No. 22ZR1419100), the National Natural Science Foundation of China Key Program (Grant No. 62132005), and CAAI-Huawei MindSpore Open Fund (Grant No. CAAIXSJLJJ-2022-005A).

REFERENCES

- [1] B. McMahan, E. Moore, D. Ramage, S. Hampson, and B. A. y Arcas, “Communication-efficient learning of deep networks from decentralized data,” pp. 1273–1282, 2017.
- [2] L. Zhu, Z. Liu, and S. Han, “Deep leakage from gradients,” *Advances in neural information processing systems*, vol. 32, 2019.

[3] C. Song, T. Ristenpart, and V. Shmatikov, “Machine learning models that remember too much,” pp. 587–601, 2017.

[4] L. Melis, C. Song, E. D. Cristofaro, and V. Shmatikov, “Exploiting unintended feature leakage in collaborative learning,” *ieee symposium on security and privacy*, 2022.

[5] A. Koskela and A. Honkela, “Learning rate adaptation for differentially private stochastic gradient descent,” 2018.

[6] L. T. Phong, Y. Aono, T. Hayashi, L. Wang, and S. Moriai, “Privacy-preserving deep learning: Revisited and enhanced,” *International Conference on Applications and Techniques in Information Security*, 2017.

[7] B. Jayaraman and D. Evans, “Evaluating differentially private machine learning in practice,” in *28th USENIX Security Symposium (USENIX Security 19)*, 2019, pp. 1895–1912.

[8] L. Xiang, J. Yang, and B. Li, “Differentially-private deep learning from an optimization perspective,” *International Conference on Computer Communications*, 2019.

[9] T. Li, A. K. Sahu, M. Zaheer, M. Sanjabi, A. Talwalkar, and V. Smith, “Federated optimization in heterogeneous networks,” *Proceedings of Machine learning and systems*, vol. 2, pp. 429–450, 2020.

[10] J. Wang, Q. Liu, H. Liang, G. Joshi, and H. V. Poor, “Tackling the objective inconsistency problem in heterogeneous federated optimization,” *Advances in neural information processing systems*, vol. 33, pp. 7611–7623, 2020.

[11] S. Wang, T. Tuor, T. Salonidis, K. K. Leung, C. Makaya, T. He, and K. Chan, “Adaptive federated learning in resource constrained edge computing systems,” *IEEE J. Sel. Areas Commun.*, vol. 37, no. 6, pp. 1205–1221, 2019.

[12] H. B. McMahan, D. Ramage, K. Talwar, and L. Zhang, “Learning differentially private recurrent language models,” *Learning*, 2017.

[13] E. Ullah, C. A. Choquette-Choo, P. Kairouz, and S. Oh, “Private federated learning with autotuned compression,” in *International Conference on Machine Learning*. PMLR, 2023, pp. 34 668–34 708.

[14] Y. Zhou, R. Wang, J. Liu, D. Wu, S. Yu, and Y. Wen, “Exploring the practicality of differentially private federated learning: A local iteration tuning approach,” *IEEE Transactions on Dependable and Secure Computing*, 2023.

[15] M. Abadi, A. Chu, I. Goodfellow, H. B. McMahan, I. Mironov, K. Talwar, and L. Zhang, “Deep learning with differential privacy,” *computer and communications security*, 2016.

[16] X. Wu, F. Li, A. Kumar, K. Chaudhuri, S. Jha, and J. F. Naughton, “Bolt-on differential privacy for scalable stochastic gradient descent-based analytics,” *international conference on management of data*, 2016.

[17] J. Fu, Z. Chen, and X. Han, “Adap dp-fl: Differentially private federated learning with adaptive noise,” in *2022 IEEE International Conference on Trust, Security and Privacy in Computing and Communications (TrustCom)*. IEEE, 2022, pp. 656–663.

[18] R. Kerkouche, G. Ács, C. Castelluccia, and P. Genevès, “Constrained differentially private federated learning for low-bandwidth devices,” in *Uncertainty in Artificial Intelligence*. PMLR, 2021, pp. 1756–1765.

[19] K. Wei, J. Li, M. Ding, C. Ma, H. Su, B. Zhang, and H. V. Poor, “User-level privacy-preserving federated learning: Analysis and performance optimization,” *IEEE Transactions on Mobile Computing*, 2021.

[20] Y. Zhou, X. Liu, Y. Fu, D. Wu, C. Li, and S. Yu, “Optimizing the numbers of queries and replies in federated learning with differential privacy,” *arXiv preprint arXiv:2107.01895*, 2021.

[21] S. Lee, T. Zhang, and A. S. Avestimehr, “Layer-wise adaptive model aggregation for scalable federated learning,” in *Proceedings of the AAAI Conference on Artificial Intelligence*, vol. 37, no. 7, 2023, pp. 8491–8499.

[22] K. Jayaram, V. Muthusamy, G. Thomas, A. Verma, and M. Purcell, “Adaptive aggregation for federated learning,” in *2022 IEEE International Conference on Big Data (Big Data)*. IEEE, 2022, pp. 180–185.

[23] S. Reddi, Z. Charles, M. Zaheer, Z. Garrett, K. Rush, J. Konečný, S. Kumar, and H. B. McMahan, “Adaptive federated optimization,” *arXiv preprint arXiv:2003.00295*, 2020.

[24] B. Karimi, P. Li, and X. Li, “Layer-wise and dimension-wise locally adaptive federated learning,” *arXiv preprint arXiv:2110.00532*, 2021.

[25] B. Zhao, B. Lyu, R. C. Fernandez, and M. Kolar, “Addressing budget allocation and revenue allocation in data market environments using an adaptive sampling algorithm,” *arXiv preprint arXiv:2306.02543*, 2023.

[26] C. Dwork, A. Roth *et al.*, “The algorithmic foundations of differential privacy,” *Foundations and Trends® in Theoretical Computer Science*, vol. 9, no. 3–4, pp. 211–407, 2014.

[27] M. Hong, X. Chen, and Z. S. Wu, “Understanding gradient clipping in private sgd: A geometric perspective,” *neural information processing systems*, 2020.

[28] Z. Bu, Y.-X. Wang, S. Zha, and G. Karypis, “Automatic clipping: Differentially private deep learning made easier and stronger,” *arXiv preprint arXiv:2206.07136*, 2022.

[29] X. Yang, H. Zhang, W. Chen, and T.-Y. Liu, “Normalized/clipped sgd with perturbation for differentially private non-convex optimization,” *arXiv preprint arXiv:2206.13033*, 2022.

[30] T. Xia, S. Shen, S. Yao, X. Fu, K. Xu, X. Xu, and X. Fu, “Differentially private learning with per-sample adaptive clipping,” in *Proceedings of the AAAI Conference on Artificial Intelligence*, vol. 37, no. 9, 2023, pp. 10 444–10 452.

[31] J. Fu, Q. Ye, H. Hu, Z. Chen, L. Wang, K. Wang, and X. Ran, “Dp-sur: Accelerating differentially private stochastic gradient descent using selective update and release,” *arXiv preprint arXiv:2311.14056*, 2023.

[32] H. B. McMahan, E. Moore, D. Ramage, and B. A. y Arcas, “Federated learning of deep networks using model averaging,” *arXiv preprint arXiv:1602.05629*, vol. 2, 2016.

[33] G. S. Watson, “Smooth regression analysis,” *Sankhyā: The Indian Journal of Statistics, Series A*, pp. 359–372, 1964.

[34] E. S. Polovinkin, “Strongly convex analysis,” *Sbornik: Mathematics*, vol. 187, no. 2, p. 259, 1996.

[35] M. Noble, A. Bellet, and A. Dieuleveut, “Differentially private federated learning on heterogeneous data,” *arXiv: Learning*, 2021.

[36] X. Li, K. Huang, W. Yang, S. Wang, and Z. Zhang, “On the convergence of fedavg on non-iid data,” *CoRR*, vol. abs/1907.02189, 2019.

[37] I. Mironov, “Rényi differential privacy,” *ieee computer security foundations symposium*, 2017.

[38] I. Mironov, K. Talwar, and L. Zhang, “Rényi differential privacy of the sampled gaussian mechanism,” *arXiv: Learning*, 2019.

[39] X. Shen, Y. Liu, and Z. Zhang, “Performance-enhanced federated learning with differential privacy for internet of things,” *IEEE Internet of Things Journal*, vol. 9, no. 23, pp. 24 079–24 094, 2022.

[40] Y. LeCun, L. Bottou, Y. Bengio, and P. Haffner, “Gradient-based learning applied to document recognition,” *Proceedings of the IEEE*, vol. 86, no. 11, pp. 2278–2324, 1998.

[41] H. Xiao, K. Rasul, and R. Vollgraf, “Fashion-mnist: a novel image dataset for benchmarking machine learning algorithms,” *arXiv preprint arXiv:1708.07747*, 2017.

[42] A. Krizhevsky, “Learning multiple layers of features from tiny images,” 2009.

[43] T. Lin, L. Kong, S. U. Stich, and M. Jaggi, “Ensemble distillation for robust model fusion in federated learning,” *Advances in Neural Information Processing Systems*, vol. 33, pp. 2351–2363, 2020.

[44] H. Yu, S. Yang, and S. Zhu, “Parallel restarted sgd with faster convergence and less communication: Demystifying why model averaging works for deep learning,” in *Proceedings of the AAAI Conference on Artificial Intelligence*, vol. 33, no. 01, 2019, pp. 5693–5700.

[45] A. Khaled, K. Mishchenko, and P. Richtárik, “Tighter theory for local sgd on identical and heterogeneous data,” in *International Conference on Artificial Intelligence and Statistics*. PMLR, 2020, pp. 4519–4529.

[46] S. P. Karimireddy, S. Kale, M. Mohri, S. Reddi, S. Stich, and A. T. Suresh, “Scaffold: Stochastic controlled averaging for federated learning,” in *International conference on machine learning*. PMLR, 2020, pp. 5132–5143.

[47] S. U. Stich, “Local sgd converges fast and communicates little,” *arXiv preprint arXiv:1805.09767*, 2018.

APPENDIX

A. Proof of Theorem 1

For the sake of convenience, we first establish some notations:

Let \mathbf{w}_t^i represent the model of the i -th client at the t -th iteration. Let \mathcal{I}_τ denote the global aggregation step, which is defined as $\mathcal{I}_\tau = \{n\tau | n = 1, 2, \dots\}$. Based on Assumption 3, the gradient descent equation can be expressed as:

$$\mathbf{v}_{t+1}^i = \mathbf{w}_t^i - \frac{\eta}{|\mathcal{B}_t^i|} \left(\sum_{s \in \mathcal{B}_t^i} \nabla F_i(\mathbf{w}_t^i, s) + \sigma C \mathcal{N}(0, \mathbf{I}_d) \right) \quad (17)$$

$$\mathbf{w}_{t+1}^i = \begin{cases} \mathbf{v}_{t+1}^i & \text{if } t+1 \notin \mathcal{I}_\tau, \\ \sum_{i=1}^N p_i \mathbf{v}_{t+1}^i & \text{if } t+1 \in \mathcal{I}_\tau. \end{cases} \quad (18)$$

Here, we introduce \mathbf{v}_{t+1}^i to represent the intermediate result of \mathbf{w}_t^i after one iteration of gradient descent.

Inspired by [47], we introduce two virtual sequences in our analysis: $\bar{\mathbf{v}}_t = \sum_{i=1}^N p_i \mathbf{v}_t^i$ and $\bar{\mathbf{w}}_t = \sum_{i=1}^N p_i \mathbf{w}_t^i$. When $t+1 \notin \mathcal{I}_\tau$, $\bar{\mathbf{v}}_t = \bar{\mathbf{w}}_t$, but the server cannot access these two sequences. When $t+1 \in \mathcal{I}_\tau$, the server can access $\bar{\mathbf{w}}_t$.

Therefore, we have:

$$\bar{\mathbf{v}}_{t+1} = \bar{\mathbf{w}}_t - \eta \sum_{i=1}^N \frac{1}{|\mathcal{B}_t^i|} \left(\sum_{s \in \mathcal{B}_t^i} \nabla F_i(\mathbf{w}_t^i, s) + \sigma C \mathcal{N}(0, \mathbf{I}_d) \right) \quad (19)$$

1) Key lemma:

Lemma 4: (Results of one iteration). Assume Assumption 1-3, we have:

$$\mathbb{E} \|\bar{\mathbf{v}}_{t+1} - \mathbf{w}^*\|^2 \leq (1 - \eta\mu) \mathbb{E} \|\bar{\mathbf{w}}_t - \mathbf{w}^*\|^2 + \eta^2 A$$

since $\Delta_t = \mathbb{E} \|\bar{\mathbf{w}}_t - \mathbf{w}^*\|^2$, we have:

$$\Delta_{t+1} \leq (1 - \eta\mu) \Delta_t + \eta^2 A$$

where $A = (\tau - 1)^2(2 + \eta\mu) \left(C^2 + \frac{\sigma^2 C^2 d}{\hat{B}^2} \right) + 3C^2 + \frac{2\Gamma}{\eta} + \frac{\sigma^2 C^2 d}{\hat{B}^2}$, $\Gamma = F^* - \sum_{i=1}^N p_i F_i^*$.

We use mathematical induction to obtain $\Delta_t \leq \frac{v}{t}$ where $v = \max\{\frac{\beta^2 + A}{\beta\mu - 1}, \tau\Delta_1\}$.

STEP 1. When $t = 1$, the equation $\Delta_1 \leq v$ holds obviously.

STEP 2. We assume $\Delta_t \leq \frac{v}{t}$ holds.

STEP 3. on the condition that $\eta = \frac{\beta}{t}$, $\beta > \frac{1}{\mu}$, we know

$$\begin{aligned} \Delta_{t+1} &\leq (1 - \eta\mu) \Delta_t + \eta^2 A \\ &\leq \left(1 - \frac{\beta\mu}{t}\right) \frac{v}{t} + \frac{\beta^2 + A}{t^2} \\ &= \frac{(t-1)v}{t^2} + \left(\frac{\beta^2 + A}{t^2} - \frac{\beta\mu - 1}{t^2} v\right) \\ &\leq \frac{t-1}{t^2} v \leq \frac{v}{t+1} \end{aligned}$$

Therefore, $\Delta_{t+1} \leq \frac{v}{t+1}$ holds, completing the proof by mathematical induction. Hence, $\Delta_t \leq \frac{v}{t}$ holds.

Then by the L -smoothness of $F(\cdot)$, and set $\beta = \frac{2}{\mu}$, $t \leftarrow T$

$$\begin{aligned} \mathbb{E}[F(\bar{\mathbf{w}}_T)] - F^* &\leq \frac{L}{2} \Delta_T \\ &\leq \frac{L}{2T} \left(\frac{4}{\mu^2} + A + \tau\Delta_1 \right) \\ &\leq \frac{L}{2T} \left(\frac{4}{\mu^2} + \tau\Delta_1 + (\tau - 1)^2(2 + \eta\mu) \left(C^2 + \frac{\sigma^2 C^2 d}{\hat{B}^2} \right) \right. \\ &\quad \left. + 3C^2 + \frac{2\Gamma}{\eta} + \frac{\sigma^2 C^2 d}{\hat{B}^2} \right) \\ &= \frac{L(2 + \eta\mu) \left(C^2 + \frac{\sigma^2 C^2 d}{\hat{B}^2} \right)}{2T} (\tau - 1)^2 \\ &\quad + \frac{L}{2T} \left(\frac{4}{\mu^2} + \tau\Delta_1 + 3C^2 + \frac{2\Gamma}{\eta} + \frac{\sigma^2 C^2 d}{\hat{B}^2} \right) \\ &= h(\tau) \end{aligned} \quad (20)$$

where

$$\begin{aligned} h(\tau) &\triangleq \frac{L(2 + \eta\mu) \left(C^2 + \frac{\sigma^2 C^2 d}{\hat{B}^2} \right)}{2T} \tau^2 \\ &\quad + \frac{L\Delta_1 - 2L(2 + \eta\mu) \left(C^2 + \frac{\sigma^2 C^2 d}{\hat{B}^2} \right)}{2T} \tau + \\ &\quad \frac{L \left((2 + \eta\mu) \left(C^2 + \frac{\sigma^2 C^2 d}{\hat{B}^2} \right) + \frac{4}{\mu^2} + 3C^2 + \frac{2\Gamma}{\eta} + \frac{\sigma^2 C^2 d}{\hat{B}^2} \right)}{2T} \end{aligned} \quad (21)$$

2) Proof of Lemma 4:

According to (17),

$$\begin{aligned}
& \|\bar{\mathbf{v}}_{t+1} - \mathbf{w}^*\|^2 \\
&= \|\bar{\mathbf{w}}_t - \mathbf{w}^* \\
&\quad - \eta \sum_{i=1}^N p_i \frac{1}{|\mathcal{B}_t^i|} \left(\sum_{s \in \mathcal{B}_t^i} \nabla F_i(\mathbf{w}_t^i, s) + \sigma C \mathcal{N}(0, \mathbf{I}_d) \right) \|^2 \\
&= \|\bar{\mathbf{w}}_t - \mathbf{w}^*\|^2 \\
&\quad + \underbrace{2\eta \langle \mathbf{w}^* - \bar{\mathbf{w}}_t, \sum_{i=1}^N p_i \frac{1}{|\mathcal{B}_t^i|} \left(\sum_{s \in \mathcal{B}_t^i} \nabla F_i(\mathbf{w}_t^i, s) + \sigma C \mathcal{N}(0, \mathbf{I}_d) \right) \rangle}_{\mathcal{A}_1} \\
&\quad + \underbrace{\eta^2 \left\| \sum_{i=1}^N p_i \frac{1}{|\mathcal{B}_t^i|} \left(\sum_{s \in \mathcal{B}_t^i} \nabla F_i(\mathbf{w}_t^i, s) + \sigma C \mathcal{N}(0, \mathbf{I}_d) \right) \right\|^2}_{\mathcal{A}_2}
\end{aligned} \tag{22}$$

By the convexity of $\|\cdot\|^2$,

$$\begin{aligned}
\mathcal{A}_1 &= -\langle \bar{\mathbf{w}}_t - \mathbf{w}^*, \sum_{i=1}^N p_i \frac{1}{|\mathcal{B}_t^i|} \left(\sum_{s \in \mathcal{B}_t^i} \nabla F_i(\mathbf{w}_t^i, s) + \sigma C \mathcal{N}(0, \mathbf{I}_d) \right) \rangle \\
&= \underbrace{-\langle \bar{\mathbf{w}}_t - \mathbf{w}^*, \sum_{i=1}^N p_i \frac{1}{|\mathcal{B}_t^i|} \sum_{s \in \mathcal{B}_t^i} \nabla F_i(\mathbf{w}_t^i, s) \rangle}_{\mathcal{B}_1} \\
&\quad - \underbrace{\langle \bar{\mathbf{w}}_t - \mathbf{w}^*, \sum_{i=1}^N p_i \frac{1}{|\mathcal{B}_t^i|} \sigma C \mathcal{N}(0, \mathbf{I}_d) \rangle}_{\mathcal{B}_2}
\end{aligned}$$

Because the noise has a mean of 0:

$$\mathbb{E} \mathcal{B}_2 = 0 \tag{23}$$

Add a zero term to \mathcal{B}_1 :

$$\begin{aligned}
\mathcal{A}_2 &= \left\| \sum_{i=1}^N p_i \frac{1}{|\mathcal{B}_t^i|} \left(\sum_{s \in \mathcal{B}_t^i} \nabla F_i(\mathbf{w}_t^i, s) + \sigma C \mathcal{N}(0, \mathbf{I}_d) \right) \right\|^2 \\
&\leq \sum_{i=1}^N p_i \left\| \frac{1}{|\mathcal{B}_t^i|} \left(\sum_{s \in \mathcal{B}_t^i} \nabla F_i(\mathbf{w}_t^i, s) + \sigma C \mathcal{N}(0, \mathbf{I}_d) \right) \right\|^2 \\
&\leq \sum_{i=1}^N p_i \left\| \frac{1}{|\mathcal{B}_t^i|} \sum_{s \in \mathcal{B}_t^i} \nabla F_i(\mathbf{w}_t^i, s) \right\|^2 \\
&\quad + \sum_{i=1}^N p_i \left\| \frac{1}{|\mathcal{B}_t^i|} \sigma C \mathcal{N}(0, \mathbf{I}_d) \right\|^2
\end{aligned}$$

(From the Cauchy Schwartz inequality.)

Take the expectation of \mathcal{A}_2 :

$$\mathbb{E} \mathcal{A}_2 \leq C^2 + \frac{\sigma^2 C^2 d}{\hat{B}^2}$$

where $\frac{1}{\hat{B}} = \max_{i,t} \mathbb{E} \frac{1}{|\mathcal{B}_t^i|}$.

By Cauchy-Schwarz inequality and AM-GM inequality, we have

$$\begin{aligned}
\mathcal{C}_1 &\leq \frac{1}{\eta} \sum_{i=1}^N p_i \|\bar{\mathbf{w}}_t - \mathbf{w}_t^i\|^2 + \eta \sum_{i=1}^N p_i \left\| \frac{1}{|\mathcal{B}_t^i|} \sum_{s \in \mathcal{B}_t^i} \nabla F_i(\mathbf{w}_t^i, s) \right\|^2 \\
&\leq \frac{1}{\eta} \sum_{i=1}^N p_i \|\bar{\mathbf{w}}_t - \mathbf{w}_t^i\|^2 + \eta C^2
\end{aligned}$$

According to Assumption 2, we get

$$\begin{aligned}
\mathcal{C}_2 &\leq -\sum_{i=1}^N p_i \langle \mathbf{w}_t^i - \mathbf{w}^*, \frac{1}{|\mathcal{B}_t^i|} \sum_{s \in \mathcal{B}_t^i} \nabla F_i(\mathbf{w}_t^i, s) \rangle \\
&\leq -\sum_{i=1}^N p_i (F_i(\mathbf{w}_t^i) - F_i(\mathbf{w}^*)) - \sum_{i=1}^N p_i \frac{\mu}{2} \|\mathbf{w}_t^i - \mathbf{w}^*\|^2 \\
&= -\sum_{i=1}^N p_i (F_i(\mathbf{w}_t^i) - F(\mathbf{w}^*) + F(\mathbf{w}^*) - F_i(\mathbf{w}^*)) \\
&\quad - \frac{\mu}{2} \sum_{i=1}^N p_i \|\mathbf{w}_t^i - \mathbf{w}^*\|^2 \\
&= -\sum_{i=1}^N p_i (F_i(\mathbf{w}_t^i) - F(\mathbf{w}^*)) + \sum_{i=1}^N p_i (F_i(\mathbf{w}^*) - F(\mathbf{w}^*)) \\
&\quad - \frac{\mu}{2} \sum_{i=1}^N p_i \|\mathbf{w}_t^i - \mathbf{w}^*\|^2 \\
&\leq \underbrace{-\sum_{i=1}^N p_i (F_i(\mathbf{w}_t^i) - F(\mathbf{w}^*))}_{\mathcal{D}_1} - \frac{\mu}{2} \sum_{i=1}^N p_i \|\mathbf{w}_t^i - \mathbf{w}^*\|^2 + \Gamma
\end{aligned}$$

where $\Gamma \triangleq \sum_{i=1}^N p_i (F(\mathbf{w}^*) - F_i(\mathbf{w}^*))$.

Process the \mathcal{D}_1

$$\begin{aligned}
\mathcal{D}_1 &= \sum_{i=1}^N p_i (F_i(\mathbf{w}_t^i) - F(\mathbf{w}^*)) \\
&= \sum_{i=1}^N p_i (F_i(\mathbf{w}_t^i) - F_i(\bar{\mathbf{w}}_t)) + \sum_{i=1}^N p_i (F_i(\bar{\mathbf{w}}_t) - F(\mathbf{w}^*)) \\
&\geq \sum_{i=1}^N p_i \langle \nabla F_i(\bar{\mathbf{w}}_t), \mathbf{w}_t^i - \bar{\mathbf{w}}_t \rangle + (F(\bar{\mathbf{w}}_t) - F(\mathbf{w}^*))
\end{aligned}$$

(from the Assumption 2)

$$\begin{aligned}
&\geq -\frac{1}{2} \sum_{i=1}^N p_i \left[\eta \|\nabla F_i(\bar{\mathbf{w}}_t)\|^2 + \frac{1}{\eta} \|\mathbf{w}_t^i - \bar{\mathbf{w}}_t\|^2 \right] \\
&\quad + (F(\bar{\mathbf{w}}_t) - F(\mathbf{w}^*))
\end{aligned}$$

(from the AM-GM inequality)

$$\begin{aligned}
&\geq -\sum_{i=1}^N p_i \left[\eta L (F_i(\bar{\mathbf{w}}_t) - F(\mathbf{w}^*)) + \frac{1}{2\eta} \|\mathbf{w}_t^i - \bar{\mathbf{w}}_t\|^2 \right] \\
&\quad + (F(\bar{\mathbf{w}}_t) - F(\mathbf{w}^*))
\end{aligned}$$

(from the Assumption 1)

$$= (1 - \eta L) (F(\bar{\mathbf{w}}_t) - F(\mathbf{w}^*)) + \frac{1}{2\eta} \sum_{i=1}^N p_i \|\mathbf{w}_t^i - \bar{\mathbf{w}}_t\|^2$$

Hence, we get

$$\begin{aligned}
\mathcal{B}_1 &\leq \frac{1}{\eta} \sum_{i=1}^N p_i \|\bar{\mathbf{w}}_t - \mathbf{w}_t^i\|^2 + \eta C^2 \\
&\quad + (\eta L - 1) (F(\bar{\mathbf{w}}_t) - F(\mathbf{w}^*)) - \frac{1}{2\eta} \|\mathbf{w}_t^i - \bar{\mathbf{w}}_t\|^2 \\
&\quad - \frac{\mu}{2} \sum_{i=1}^N p_i \|\mathbf{w}_t^i - \mathbf{w}^*\|^2 + \Gamma \\
&\leq -\frac{\mu}{2} \|\bar{\mathbf{w}}_t - \mathbf{w}^*\|^2 + \left(\frac{1}{\eta} + \frac{\mu}{2} \right) \sum_{i=1}^N p_i \|\bar{\mathbf{w}}_t - \mathbf{w}_t^i\|^2 + \eta C^2 + \Gamma
\end{aligned}$$

Comprehensive equation $\mathcal{A} - \mathcal{D}$, take exception to (22):

$$\begin{aligned}
&\mathbb{E} \|\bar{\mathbf{v}}_{t+1} - \mathbf{w}^*\|^2 = \mathbb{E} \|\bar{\mathbf{w}}_t - \mathbf{w}^*\|^2 + 2\eta \mathbb{E} \mathcal{A}_1 + \eta^2 \mathbb{E} \mathcal{A}_2 \\
&\leq \mathbb{E} \|\bar{\mathbf{w}}_t - \mathbf{w}^*\|^2 + \eta^2 \left(C^2 + \frac{\sigma^2 C^2 d}{\hat{B}^2} \right) \\
&\quad + 2\eta \left(-\frac{\mu}{2} \mathbb{E} \|\bar{\mathbf{w}}_t - \mathbf{w}^*\|^2 \right. \\
&\quad \left. + \left(\frac{1}{\eta} + \frac{\mu}{2} \right) \sum_{i=1}^N p_i \mathbb{E} \|\bar{\mathbf{w}}_t - \mathbf{w}_t^i\|^2 + \eta C^2 + \Gamma \right) \\
&= (1 - \eta\mu) \mathbb{E} \|\bar{\mathbf{w}}_t - \mathbf{w}^*\|^2 + (2 + \eta\mu) \sum_{i=1}^N p_i \mathbb{E} \|\bar{\mathbf{w}}_t - \mathbf{w}_t^i\|^2 \\
&\quad + 3\eta^2 C^2 + 2\eta\Gamma + \frac{\eta^2 \sigma^2 C^2 d}{\hat{B}^2}
\end{aligned} \tag{24}$$

Then we do such process:

$$\begin{aligned}
&\sum_{i=1}^N p_i \mathbb{E} \|\bar{\mathbf{w}}_t - \mathbf{w}_t^i\|^2 \\
&= \sum_{i=1}^N p_i \mathbb{E} \|(\mathbf{w}_t^i - \bar{\mathbf{w}}_{t_0}) - (\bar{\mathbf{w}}_t - \bar{\mathbf{w}}_{t_0})\|^2 \\
&\leq \sum_{i=1}^N p_i \mathbb{E} \sum_{t=t_0}^{t-1} (\tau - 1) \eta^2 \left\| \frac{1}{|\mathcal{B}_t^i|} \left(\sum_{s \in \mathcal{B}_t^i} \nabla F_i(\mathbf{w}_t^i, s) + \sigma \mathcal{N}(0, \mathbf{I}_d) \right) \right\|^2 \\
&\leq \sum_{i=1}^N p_i \eta^2 (\tau - 1)^2 \left(\mathbb{E} \left\| \frac{1}{|\mathcal{B}_t^i|} \sum_{s \in \mathcal{B}_t^i} \nabla F_i(\mathbf{w}_t^i, s) \right\|^2 + \frac{\sigma^2 C^2 d}{\hat{B}^2} \right) \\
&\leq \eta^2 (\tau - 1)^2 \left(C^2 + \frac{\sigma^2 C^2 d}{\hat{B}^2} \right)
\end{aligned} \tag{25}$$

Combine Equation (22) and Equation (25):

$$\mathbb{E} \|\bar{\mathbf{v}}_{t+1} - \mathbf{w}^*\|^2 \leq (1 - \eta\mu) \mathbb{E} \|\bar{\mathbf{w}}_t - \mathbf{w}^*\|^2 + \eta A \tag{26}$$

where

$$A = (\tau - 1)^2 (2 + \eta\mu) \left(C^2 + \frac{\sigma^2 C^2 d}{\hat{B}^2} + 3C^2 + \frac{2\Gamma}{\eta} + \frac{\sigma^2 C^2 d}{\hat{B}^2} \right) \tag{27}$$